Glioma tumor suppressor candidate region gene 1 (GLTSCR1) and its paralog GLTSCR1-like form SWI/SNF chromatin remodeling subcomplexes

Received for publication, November 22, 2017, and in revised form, January 24, 2018 Published, Papers in Press, January 26, 2018, DOI 10.1074/jbc.RA117.001065

Aktan Alpsoy and Emily C. Dykhuizen[1]

From the Department of Medicinal Chemistry and Molecular Pharmacology, Purdue University, West Lafayette, Indiana 47907

Edited by Joel Gottesfeld

The mammalian SWI/SNF chromatin remodeling complex is a heterogeneous collection of related protein complexes required for gene regulation and genome integrity. It contains a central ATPase (BRM or BRG1) and various combinations of 10–14 accessory subunits (BAFs for BRM/BRG1 Associated Factors). Two distinct complexes differing in size, BAF and the slightly larger polybromo-BAF (PBAF), share many of the same core subunits but are differentiated primarily by having either AT-rich interaction domain 1A/B (ARID1A/B in BAF) or ARID2 (in PBAF). Using density gradient centrifugation and immunoprecipitation, we have identified and characterized a third and smaller SWI/SNF subcomplex. We termed this complex GBAF because it incorporates two mutually exclusive paralogs, GLTSCR1 (glioma tumor suppressor candidate region gene 1) or GLTSCR1L (GLTSCR1-like), instead of an ARID protein. In addition to GLTSCR1 or GLTSCR1L, the GBAF complex contains BRD9 (bromodomain-containing 9) and the BAF subunits BAF155, BAF60, SS18, BAF53a, and BRG1/BRM. We observed that GBAF does not contain the core BAF subunits BAF45, BAF47, or BAF57. Even without these subunits, GBAF displayed *in vitro* ATPase activity and bulk chromatin affinity comparable to those of BAF. GBAF associated with BRD4, but, unlike BRD4, the GBAF component GLTSCR1 was not required for the viability of the LNCaP prostate cancer cell line. In contrast, *GLTSCR1* or *GLTSCR1L* knockouts in the metastatic prostate cancer cell line PC3 resulted in a loss in proliferation and colony-forming ability. Taken together, our results provide evidence for a compositionally novel SWI/SNF subcomplex with cell type–specific functions.

The mammalian SWI/SNF (or BAF) complex is an ATP-dependent chromatin remodeler composed of 10–14 subunits (1). The mammalian SWI/SNF chromatin remodeling complex is implicated in a variety of processes including mitosis, DNA replication, DNA damage repair, genomic looping, and gene splicing, in addition to its well-established roles in the transcriptional regulation of genes involved in cellular differentiation, cellular maintenance, and adaptation to stimuli (2). Mutations in specific SWI/SNF complex members are common in cancer (3, 4) and neural disorders (5), and the altered expression of specific subunits is associated with tumorigenesis (6), viral infection (7), viral latency (8), alcohol addiction (9, 10), heart disease (11), and immune function (12). The ability of this complex to direct such numerous and diverse functions is facilitated through the increase in SWI/SNF subunit number and diversity during vertebrate evolution (13), which led to an exponential increase in the potential combinations of subunits (14, 15). All SWI/SNF complexes contain the ATPase subunit BRG1 or BRM, along with the structural subunits BAF155/BAF170, which are required for full ATPase and nucleosome remodeling activity *in vitro* (16). In addition, SWI/SNF complexes contain BAF60 (A, B, or C), BAF47, BAF57, BAF53 (A or B), and actin. The larger and less abundant polybromo-BAF (PBAF)[2] complex uniquely contains ARID2, PBRM1, BAF45D, and BRD7, whereas the more abundant BAF complex contains ARID1 (A or B), BAF45 (B, C, or D), SS18, BCL7 (A, B, or C), and BCL11 (A or B) (Fig. 1*A*). The altered expression of SWI/SNF paralogs during cellular differentiation results in subunit switching, which is an important determinant of cell identity and cell-type transcriptional programs (17). Additionally, paralogs are often expressed simultaneously, leading to distinct subcomplexes within the same cell with both unique and redundant functions (18). For example, ARID1A is high in embryonic stem cells, whereas ARID1B is up-regulated upon differentiation (19). The different BAF complexes containing these two paralogs share many of their genomic targets; however, they also bind unique genomic targets, and deletions are non-synonymous for gene regulation (20). ARID1A is the most commonly mutated SWI/SNF subunit in cancer, because of transcriptional functions that are non-redundant with ARID1B (21, 22); however, cancers with deletions in ARID1A are dependent on ARID1B for viability (23) because of redundant, essential functions at enhancers (22). Additionally, homologous complexes can display transcriptionally antagonistic roles, as has been observed

This work was supported with National Institutes of Health Grant CA207532, V Foundation for Cancer Research Grants V2014-004 and D2016-030 (to E. C. D.), a graduate endowment from the Lilly Foundation (to A. A.), and National Institutes of Health Grant P30 CA023168 through the Purdue University Center. The authors declare that they have no conflicts of interest with the contents of this article. The content is solely the responsibility of the authors and does not necessarily represent the official views of the National Institutes of Health.

This article contains Figs. S1–S3.

[1] To whom correspondence should be addressed: Dept. of Medicinal Chemistry and Molecular Pharmacology, HANS105A, 201 S. University St., West Lafayette IN 47907. Tel.: 765-494-4706; E-mail: edykhui@purdue.edu.

[2] The abbreviations used are: PBAF, polybromo-BAF; IP, immunoprecipitation; DMEM, Dulbecco's modified Eagle's medium; MEM, minimal essential medium; qPCR, quantitative PCR; DMSO, dimethyl sulfoxide; sgRNA, short guide RNA; AML, acute myeloid leukemia; mESC, mouse embryonic stem cell.

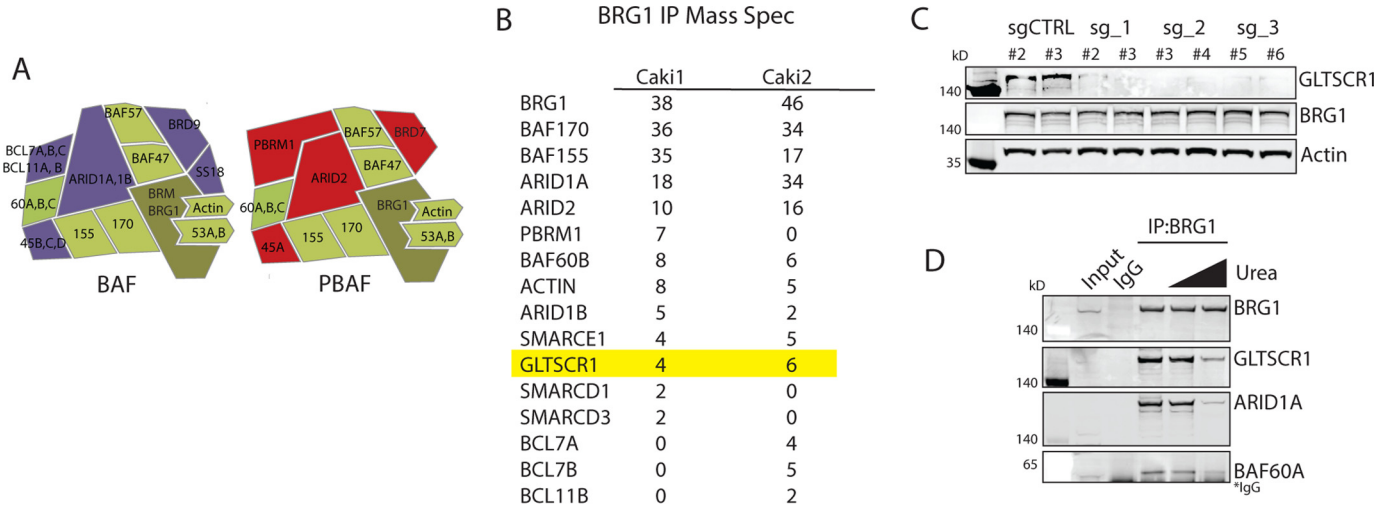

Figure 1. GLTSCR1 is a dedicated subunit of the SWI/SNF chromatin remodeling complex. *A*, current illustration of mammalian SWI/SNF complex composition. *B*, mass spectrometry (*Spec*) analysis of BRG1 IP from two human renal cancer cell lines identifies peptides from GLTSCR1. *C*, GLTSCR1 specific antibody identified using *Gltscr1* knockout mESCs derived using three different sgRNA constructs. *D*, immunoprecipitation with antibodies against BRG1 confirms GLTSCR1 association. Urea denaturation with 0.5 and 2.5 M urea prior to BRG1 immunoprecipitation indicates the strong association of GLTSCR1 to BRG1, comparable to the strength of association of BRG1 to core BAF subunits ARID1A and BAF60A.

for ARID1A and ARID2-containing complexes at specific gene targets (8, 20, 24). Targeting specific SWI/SNF complexes has been proposed both for alleviating subunit-specific pathogenic function and to target essential redundant functions in cancers with mutations in the genes for specific subunits (25, 26). Both of these strategies are dependent on a better understanding of the different biochemical and transcriptional functions of homologous SWI/SNF complexes. We report here for the first time a novel, ubiquitously expressed SWI/SNF subcomplex defined by mutually exclusive paralogs GLTSCR1 (or BICRA for BRD4-interacting chromatin remodeling complex associated) and GLTSCR1L (or BICRAL for BRD4-interacting chromatin remodeling complex associated like), which also contains BRD9 and a subset of shared canonical SWI/SNF subunits.

Results

Proteomic analysis of BRG1 immunoprecipitations from two renal clear cell carcinoma cell lines identified multiple unique peptides from the uncharacterized protein GLTSCR1 (Fig. 1*B*). GLTSCR1 has been identified in previous proteomic analyses of the SWI/SNF chromatin remodeling complex (18, 27–29) but has never been validated or characterized as a BAF complex subunit. After screening multiple commercially available antibodies against GLTSCR1, we identified an antibody that stained a band in the predicted region of 180 kDa using immunoblot analysis. Further, this band disappeared after CRISPR-mediated *Gltscr1* knockout in mouse embryonic stem cell lines (Fig. 1*C*). Using this validated antibody, we confirmed the mass spectrometry data using immunoblot analysis, detecting robust enrichment of GLTSCR1 in BRG1 immunoprecipitations (Fig. 1*D*). To define whether GLTSCR1 is a true subunit of BAF and not an associating factor, we performed urea denaturation followed by BRG1 immunoprecipitation and found that GLTSCR1 stably associates with BRG1 at urea concentrations up to 2.5 M, consistent with known BAF subunits ARID1A and BAF60A (Fig. 1*D*).

To determine which SWI/SNF subcomplex contains GLTSCR1, we performed glycerol gradient analysis to separate the two closely related SWI/SNF complexes, BAF and PBAF, based on density. Surprisingly, GLTSCR1 staining was detected in earlier gradient fractions 11–13, which did not overlap with ARID1A (a subunit exclusive to the BAF complex) in fractions 14–16 or PBRM1 (a subunit exclusive to the PBAF complex) in fractions 17–19 or with BAF47 (a subunit shared by both BAF and PBAF) (Fig. 2*A*, *left panel*). To ensure that this was not an aberrant partial complex caused by specific cancerous alterations or cell culture artifacts, we performed similar analysis in a second cell line (PC3) and observed the same pattern for GLTSCR1 (Fig. 2*A*, *right panel*). To define whether any additional SWI/SNF subunits in addition to BRG1 associate with this subcomplex, we performed a series of immunoprecipitations to various known subunits of the BAF or PBAF complex (Fig. 2*B*). From this panel, only antibodies against BRG1 and BRM were able to precipitate GLTSCR1, and as expected from the glycerol gradient analysis, GLTSCR1 did not associate with BAF-specific subunits ARID1A/ARID1B or PBAF-specific subunit PBRM1. Surprisingly, however, we did not observe GLTSCR1 association with BAF45D or BAF57, subunits thought to be canonical subunits, although we did observe association with core subunits BAF155 and BAF53a (Fig. 2*C*). Using GLTSCR1 immunoprecipitations in HEK293T cells, we further identified that BAF60A, SS18, and BRD9 are GBAF subunits, whereas BAF170 and BAF47 are not (Fig. 2*D*), which was confirmed in THP1 cells (Fig. S1*A*). Further, glycerol gradient analysis and co-immunoprecipitation experiments identified BRD9 as a subunit of GBAF but not BAF or PBAF, SS18 as a subunit shared by BAF and GBAF, and BAF170 and BAF47 as subunits exclusive to BAF and PBAF (Fig. 2, *E* and *F*). An illustration of the proposed composition of these complexes based on the immunoprecipitation experiments is depicted in Fig. 2*G*. To validate GBAF as a potential chromatin remodeling complex, we next performed ATPase assays on immunoprecipitations of

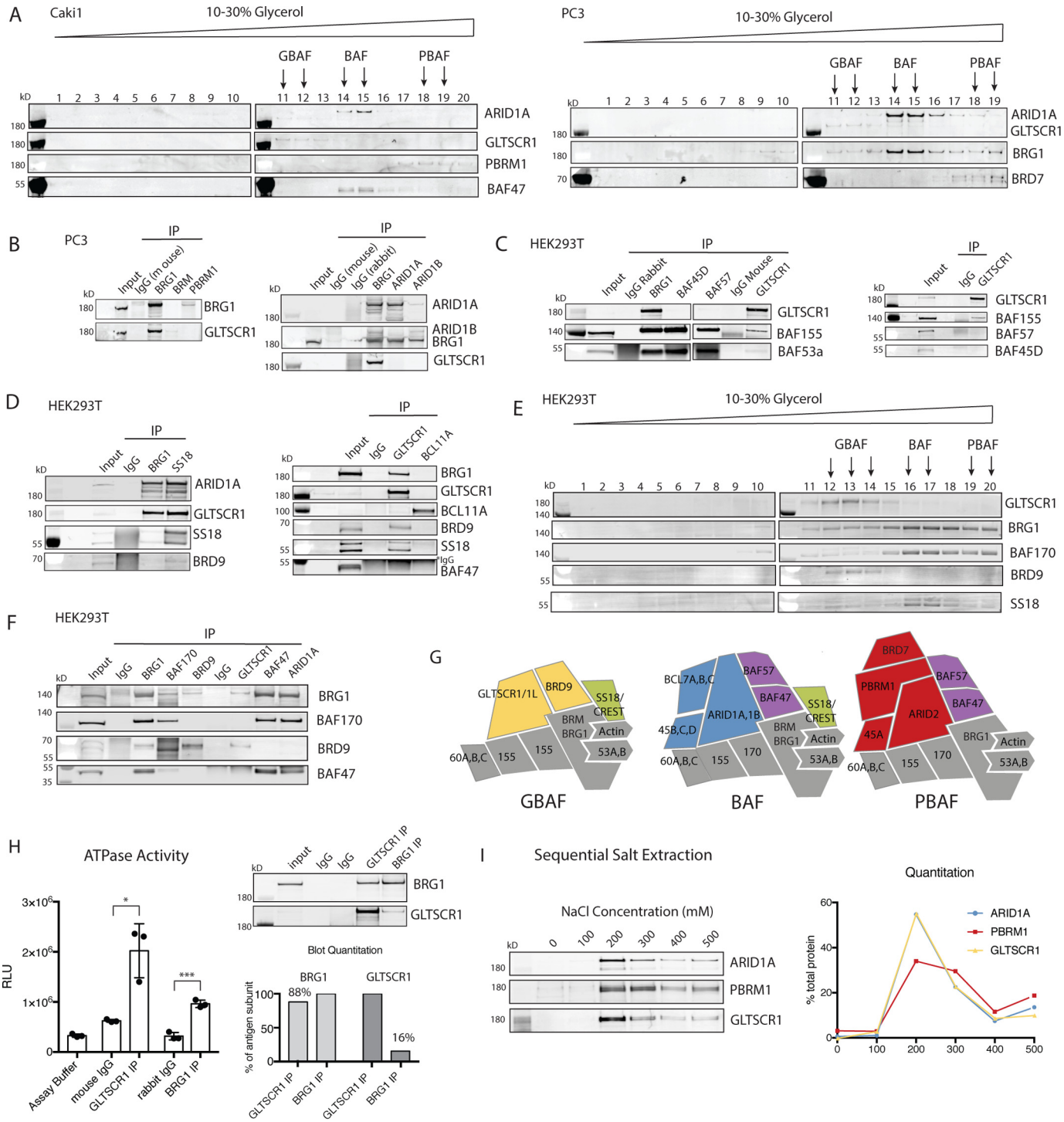

Figure 2. GLTSCR1 is in a novel SWI/SNF subcomplex GBAF. *A*, Glycerol gradients from renal cancer cell line Caki1 and prostate cancer cell line PC3 indicate that GLTSCR1 does not co-sediment with BAF subunit ARID1A or PBAF subunits PBRM1 (for Caki1) or BRD7 (for PC3). *B*, IP experiments of BAF subunits from PC3 lysates identify GLTSCR1 association with BRG1 and BRM. *C*, BAF subunit and GLTSCR1 IP experiments from HEK293T lysates identify GLTSCR1 association with BAF155 and BAF53a but not BAF47, BAF57, or BAF45D. *D*, BAF subunit and GLTSCR1 IP experiments from HEK293T lysates identify GLTSCR1 association with SS18 and BRD9 but not BCL11A. *E* and *F*, glycerol gradient analysis (*E*) and BAF subunit IP experiments (*F*) from HEK293T lysates identify GLTSCR1 association with BRG1 and SS18 but not BAF170 and BAF47 and validate BRD9 as a subunit found in GBAF, but not BAF/PBAF. *G*, schematic representation of GBAF, BAF, and PBAF composition. *Yellow* subunits are unique to GBAF, *blue* subunits are unique to BAF, *red* subunits are unique to PBAF, *green* subunits are shared by GBAF and BAF, *purple* subunits are shared by BAF and PBAF, and *gray* subunits are shared by all three complexes. Subcomplex GBAF consists of BAF60A, BRG1, BAF155, BRD9, BAF53A, and SS18. *H*, GBAF possesses ATPase activity. ATPase activity assay was performed with BRG1 and GLTSCR1 immunoprecipitations providing similar levels of BRG1. ATPase activities normalized to respective IgG isotype controls yielded comparable fold changes (3.03 ± 0.23, for BRG1 IP; 3.24 ± 0.87, for GLTSCR1 IP). *Error bars*, means ± S.D. ($n = 3$). *, $p < 0.05$; ***, $p < 0.001$. *I*, sequential salt extraction analysis and immunoblot quantitation indicates that GLTSCR1 interacts with bulk chromatin at a similar strength as ARID1A (representative of BAF) and PBRM1 (representative of PBAF).

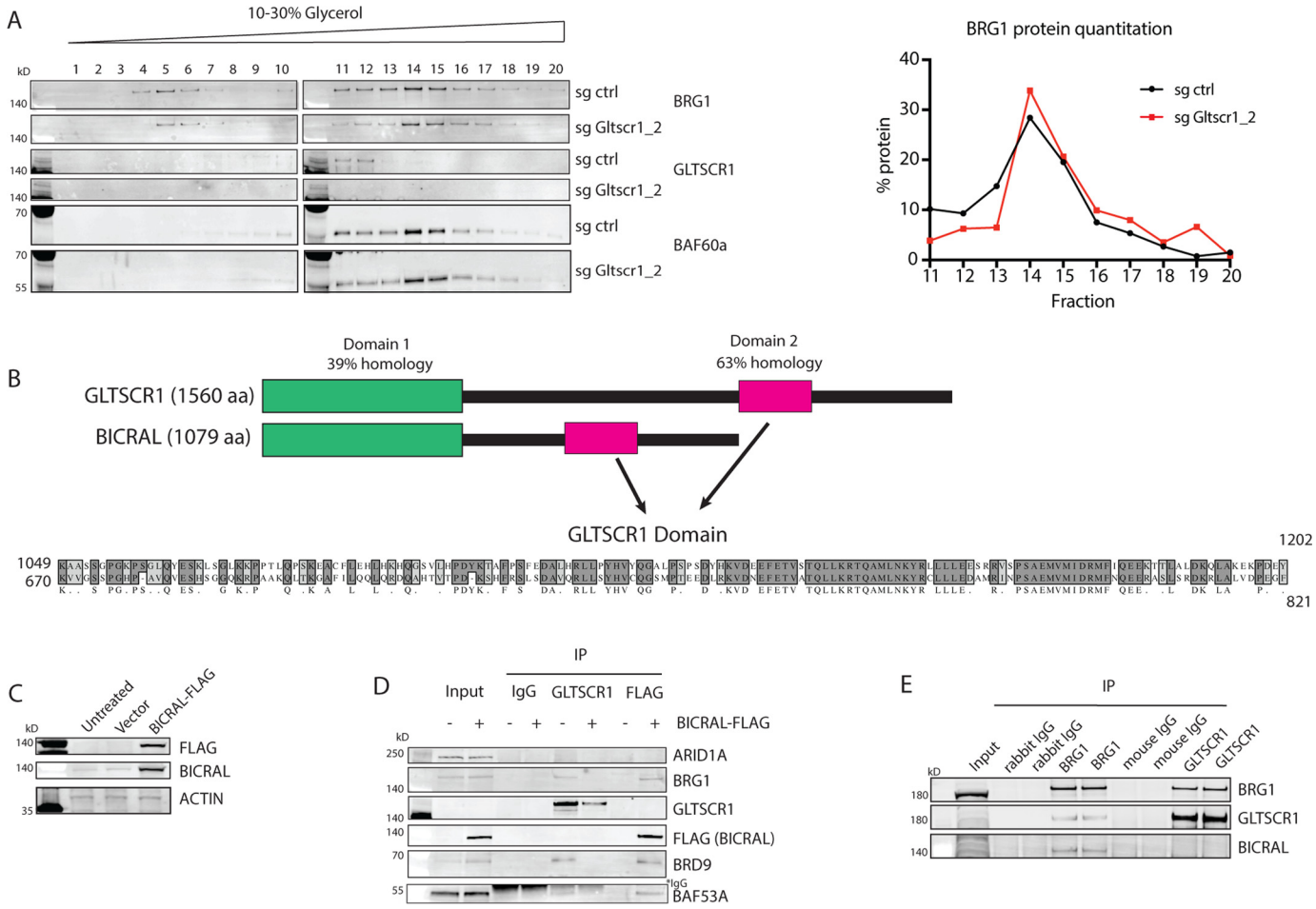

Figure 3. GBAF contains GLTSCR1 or paralog GLTSCR1L (BICRAL). *A*, glycerol gradient analysis in mESCs showing that GBAF-associated BRG1 and BAF60A were preserved in fractions 11–13 in the absence of GLTSCR1, suggesting that GBAF was not completely disrupted by *Gltscr1* knockout. *B*, pairwise alignment of amino acid sequences of GLTSCR1 and its paralog GLTSCR1L (BICRAL) show homology in the N-terminal region and strong homology at region identified at a conserved GLTSCR1 domain. *C*, verification of inducible expression of BICRAL-FLAG in HEK293T cells with both FLAG and endogenous BICRAL antibodies. *D*, immunoprecipitation analysis showed that similar to GLTSCR1, exogenous BICRAL interacts with BRD9, BAF53A, and BRG1. In addition, endogenous GLTSCR1 and BICRAL do not immunoprecipitate one another. BICRAL overexpression results in reduced GLTSCR1 protein levels. *E*, endogenous BICRAL does not associate with GLTSCR1, further validating that GLTSCR1 and BICRAL are mutually exclusive in GBAF context. BICRAL is detected in total BRG1 IP but not in GLTSCR1 IP, although both contain comparable levels of BRG1. Note that the same Western blotting is used in Fig. S1*B* to compare BRG1 levels for ATPase assay.

GLTSCR1 and BRG1 from HEK293T cells. We used GLTSCR1 immunoprecipitations containing comparable amounts of BRG1 (~90%) (Fig. 2*H* and Fig. S1*B*) and found that GBAF complexes display robust DNA-stimulated ATPase activity (Fig. 2*H*). In fact, the ATPase activity of GLTSCR1 immunoprecipitations was higher than BRG1 immunoprecipitations, although this is complicated by possible contributions from BRM, which is lowly expressed in HEK293T cells (30). We next used sequential salt extraction assays and determined that even in the absence of association with DNA-binding subunits BAF57 and ARID1/2, GLTSCR1 elutes from bulk chromatin with similar salt concentrations as BAF-specific subunit ARID1A, whereas PBAF-specific subunit PBRM1 requires slightly higher salt concentrations to elute off bulk chromatin (31) (Fig. 2*I*).

Because we established GLTSCR1 as the unique subunit of GBAF, we set to define whether GLTSCR1 is required for GBAF formation. Using GLTSCR1 knockout ES cells (Fig. 1*C*), we performed glycerol gradients with and without GLTSCR1 (Fig. 3*A*). We observed a decrease in BRG1 and BAF60A staining in GBAF fractions 11–13 but not complete loss of staining. We hypothesized that this was due to the presence of the predicted GLTSCR1 paralog, GLTSCR1L (now referred to as BICRAL for clarity), which has also been detected in BAF subunit IP mass spectrometry studies as KIAA0240 (28, 29). GLTSCR1 and BICRAL share 32% sequence homology (21% identity), and both contain a well-conserved "GLTSCR1" domain, which is also conserved between GLTSCR1 orthologs predicted in all multicellular organisms (Fig. 3*B*). We screened commercially available antibodies for BICRAL and identified one with weak staining at the predicted size of 140 kDa, along with many nonspecific bands. To confirm that the band is the correct protein, we developed a cell line with doxycycline-inducible FLAG-tagged BICRAL. Overexpression of BICRAL-FLAG in HEK293T cells resulted in a robust FLAG band at 140 kDa and an increase in staining with the endogenous antibody at the same molecular weight (Fig. 3*C*). To confirm that BICRAL is mutually exclusive with GLTSCR1 in the GBAF complex, we performed co-immunoprecipitations of GLTSCR1 and FLAG in our BICRAL-FLAG overexpression system and

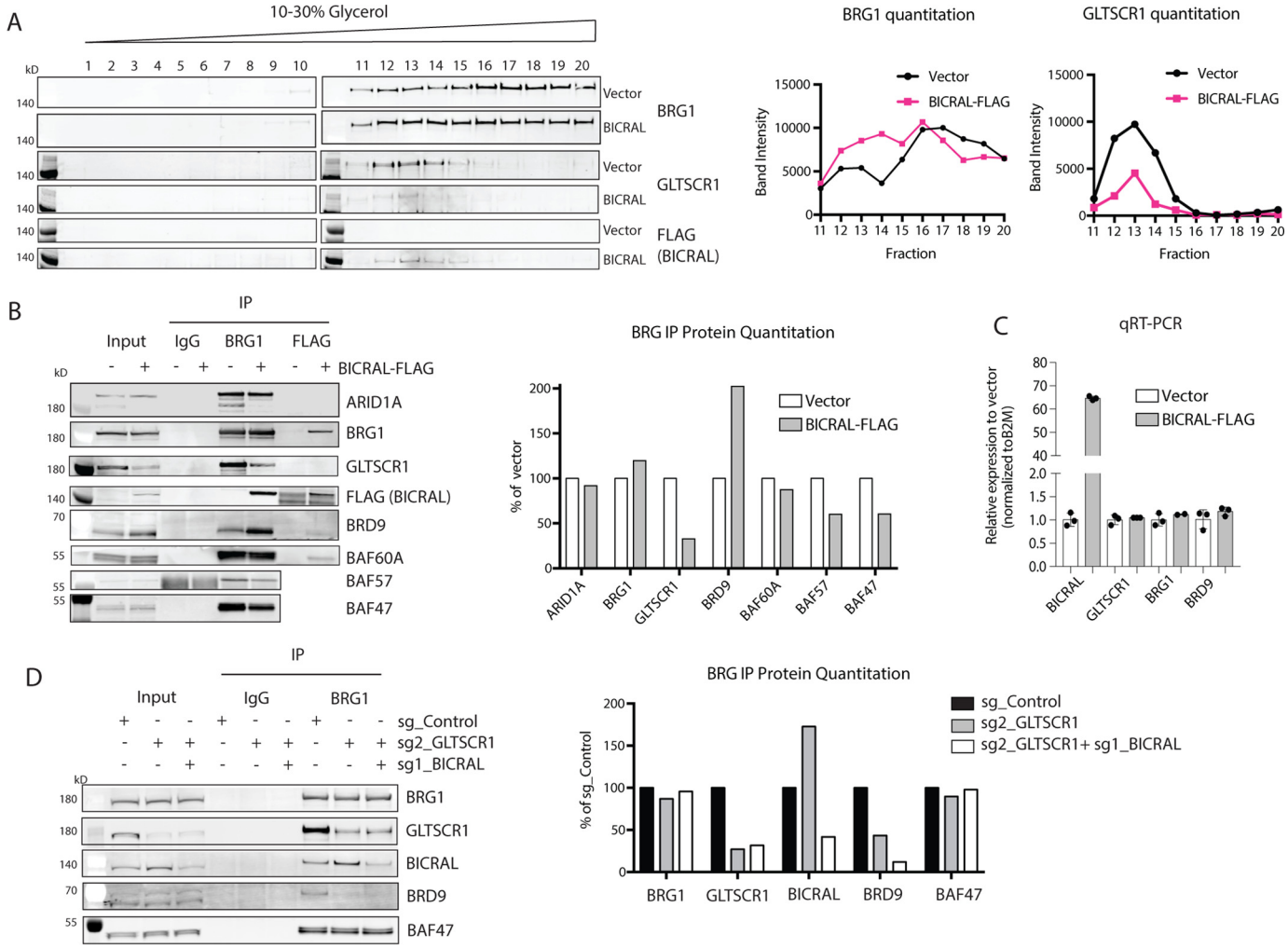

Figure 4. GLTSCR1 and BICRAL are mutually exclusive subunits of GBAF that can alter SWI/SNF complex stoichiometry. *A*, glycerol gradient analysis in BICRAL-FLAG– overexpressing HEK293T cells indicates that BICRAL is incorporated into GBAF. Overexpression of BICRAL-FLAG increases the GBAF-associated BRG1 levels (fractions 11–14), suggesting formation of new GBAF upon BICRAL overexpression. Reduced GBAF-associated GLTSCR1 levels also validate decreased GLTSCR1 protein expression upon BICRAL overexpression. *B*, immunoprecipitation analysis showing that BICRAL-FLAG overexpression reduced BRG1-associated GLTSCR1 levels and enhanced BRD9 protein levels and its association with BRG1. BICRAL-FLAG overexpression also reduced BRG1-associated BAF47 and BAF57, suggesting competition between GBAF and BAF for BRG1. *C*, RT-qPCR showing that expression of BRG1, GLTSCR1, or BRD9 did not alter upon BICRAL overexpression. *Error bars*, means ± S.D. ($n = 3$). *D*, CRISPR/Cas9-mediated knockout of *GLTSCR1* with or without CRISPR/Cas9-mediated knockout of *BICRAL* reduced the BRG1-associated BRD9 levels, as an indicator of loss of GBAF.

using endogenous proteins in HEK293T cells and found that GLTSCR1 and BICRAL do not associate with each other (Fig. 3, *D* and *E*). In addition, both GLTSCR1 and BICRAL-FLAG enrich BRG1, BAF53A, and BRD9 but not ARID1A, indicating incorporation into comparable SWI/SNF subcomplexes. Intriguingly, we also found that overexpression of BICRAL decreases GLTSCR1 expression, possibly indicating its ability to compete with and replace GLTSCR1 in GBAF complexes.

To further investigate the role of BICRAL in GBAF formation, we performed glycerol gradient analysis of BICRAL-FLAG overexpression in HEK293T cells. We found that BICRAL overexpression results in BICRAL incorporation into GBAF, as indicated by its expression in fractions 11–13, similar to the profile of GLTSCR1 staining (Fig. 4*A*). In addition, we confirmed that it is able to replace GLTSCR1 in GBAF, as indicated by an overall decrease in GLTSCR1 staining. Interestingly, we also saw an increase in BRG1 staining in fractions 11–13 upon BICRAL overexpression, indicating that BICRAL is able to alter overall SWI/SNF complex stoichiometry. To investigate this further, we performed BRG1 immunoprecipitations in the BICRAL overexpression cells. We found no changes in BRG1 expression or immunoprecipitation efficiency and confirmed the decrease in GLTSCR1 association with BRG1. In addition, we observed an increase in both the expression and the BRG1 association of BRD9 and a decrease in the BRG1 association with BAF subunits ARID1A, BAF47, and BAF57 (Fig. 4*B*). To test whether this effect is due to a transcriptional or post-translational outcome of BICRAL expression, we performed RT-qPCR in BICRAL-FLAG overexpression line and found no alterations in endogenous transcript levels for any of the subunits in question (Fig. 4*C*). This suggests that increased BRD9 protein levels and decreased GLTSCR1 levels are due to post-translational events, most likely degradation of free monomer. To confirm that GBAF is dependent on GLTSCR1 or BICRAL for formation, we also generated a double knockout HEK293T cell line. We observe that BRG1-associated BRD9 is undetect-

able in *GLTSCR1* knockout and double knockout cells, indicating loss of GBAF formation (Fig. 4*D*). It is worth noting that differences in knockout efficiencies and possibly the relative levels of GLTSCR1 and BICRAL made it difficult to distinguish additive or GLTSCR1-dominant effects of the paralogs on GBAF formation. Similar to decreased GLTSCR1 levels in BICRAL-overexpression lines, we consistently observed an increase in BICRAL levels upon *GLTSCR1* knockout (Fig. 4*D* and Fig. S3*B*) via a similar increase of protein stability through complex incorporation. This provides further evidence for a compensatory role of BICRAL for GBAF formation in the absence of GLTSCR1. These results indicate that GLTSCR1/BICRAL are mutually exclusive subunits of GBAF that can, in part, define SWI/SNF complex stoichiometry.

GLTSCR1 has also been identified in a proteomics study of BRD4-associating factors (32), as reflected by the recent change in HUGO gene name from *GLTSCR1* to *BICRA* for BRD4-Interacting Chromatin Remodeling Complex Associated protein. The BRD4 extraterminal domain was found to associate with several proteins, including NSD3 (and NSD2), ATAD5, GLTSCR1, and CHD4 (and CHD7), in an extraterminal domain-specific manner (33). Using BRD4 immunoprecipitations we confirmed that BRD4 associates with GLTSCR1, BAF155, BRD9, and BAF60A but not BAF-specific subunit BAF47 (Fig. 5*A*). Because BRD4 protein association and co-regulator activity are known to be regulated by phosphorylation (34), we treated BRD4 immunoprecipitation with alkaline phosphatase (or used phosphatase inhibitors in lysis, IP, and washes) but did not find that the association between GLTSCR1 and BRD4 is dependent on phosphorylation. We confirmed previously published findings that the androgen-sensitive prostate cancer cell line LNCaP is 10-fold more sensitive to BRD4 inhibition than androgen-insensitive prostate cancer cell line PC3 (Fig. S2*A*) (35); however, LNCaPs are not dependent on GLTSCR1 for viability (Fig. 5*B* and Fig. S2*B*). Instead, *GLTSCR1* knockout produces a small but significant increase in sensitivity to BRD4 inhibitor (Fig. 5*C* and Fig. S2*C*). To test the effect of GLTSCR1 on expression of well-characterized BRD4 target *MYCC*, we measured *MYCC* mRNA levels in the GLTSCR1 knockout in LNCaP cells and found an increase in *MYC* levels, which was reversed upon low dose (50 nM) treatment with JQ1 (Fig. 5*D*). This provides evidence that GLTSCR1 only slightly modulates BRD4 function in LNCaP cells, potentially by sequestering it from transcriptional activators such as NSD3 that are required for the activation of *MYCC* transcription by BRD4 (36).

We next performed immunoblot analysis to evaluate the expression levels of BICRAL and GLTSCR1 in a series of cell lines. We found that the majority of cell lines have similar expression of these subunits (Fig. 6*A*). *Gltscr1* knockout (Fig. 1*C*) in mouse ESCs or epithelial cell line NMuMG (Fig. S3*A*) did not affect cell viability (Fig. 6*B*). In addition, we observed no support for GLTSCR1 as a glioma tumor suppressor because *GLTSCR1* knockout in human astrocyte cell line SVG p12 and glioblastoma cell line T98G both resulted in no change in viability (Fig. 6*C* and Fig. S3*B*). Lastly, we did not find evidence that BICRAL and GLTSCR1 have redundant, necessary functions because knockout of both *GLTSCR1* and *BICRAL* in HEK293T cells did not produce any viability defect (Figs. 4*D* and 6*D*). We did, however, detect a dramatic decrease in both proliferation and colony formation upon *GLTSCR1* knockout in prostate cancer cell line PC3 (Fig. 6, *E* and *F*). We further knocked out *BICRAL* in this cell line and found similar defects in cell growth, indicating an overall dependence on GBAF function in this cell line (Fig. 6, *E* and *F*). Although PC3 cells are dependent on GLTSCR1 and BICRAL, they have low expression of BRD9 (data not shown), and are not responsive to the BRD9 inhibitor BI-7273 (Fig. 6*G*), (37), indicating that GLTSCR1 function is not always dependent on, or synonymous with, BRD9 function.

Discussion

SWI/SNF complexes play diverse roles in normal function and disease; however, most of our understanding of SWI/SNF function is from studying the ATPase subunit BRG1, which is found in multiple different SWI/SNF subcomplexes. The fact that many of the disease-related mutations are in subcomplex-specific subunits has placed increased importance in defining the composition and function of individual SWI/SNF subcomplexes. Our discovery of the ubiquitous new subcomplex GBAF, which is defined by novel subunit paralogs GLTSCR1 and BICRAL, provides another potential mechanism by which BRG1 exerts its functions. We have identified GBAF as a ubiquitously expressed SWI/SNF subcomplex with only a subset of the canonical SWI/SNF subunits but full *in vitro* ATPase activity. Gene and protein expression data indicate that these paralogs are expressed ubiquitously (30); however, knockout in many cell lines provides no immediate viability phenotype. Although this complex does not appear to be generally essential for basic cellular viability, mouse knockout data report an embryonic lethal phenotype for *Bicral* knockout animals (38). Whether these developmental roles will be shared with *Gltscr1* remains to be seen.

In contrast to the high mutation rates for subunits of the BAF and PBAF complex, subunits of GBAF (with the exception of BRG1) are not highly mutated in cancer (39). Nevertheless, our data in metastatic prostate cancer cell line PC3 suggest a possible dependence of select cancers on GLTSCR1 and/or BICRAL. Intriguingly, prostate cancers have BRG1 up-regulation, but not SNF5, and display dependences on BRG1 (40). In addition to prostate cancer, many other cancers display increased dependence on BRG1, although the associated SWI/SNF subcomplex involved in this dependence is unexplored. Inhibitors to SWI/SNF complexes have been proposed as therapies; however, inhibitors of BRG1 ATPase activity will likely have severe toxicity because of the role of BRG1 in general viability in many cell types. Therefore, the development of inhibitors to GBAF subunits may be a more promising approach. Malignant rhabdoid tumors with mutations in SNF5 are dependent on BRG1 (41), and recent reports of malignant rhabdoid tumor sensitivity to BRD9 inhibitors (42) might be due to dependence of these cancers on GBAF function, although it is possible that BRD9 can have functions outside of GBAF. Similarly, AML is dependent on SWI/SNF subunits consistent with GBAF (43), including BRD9, (37, 44) providing a potential therapeutic target in these cancers.

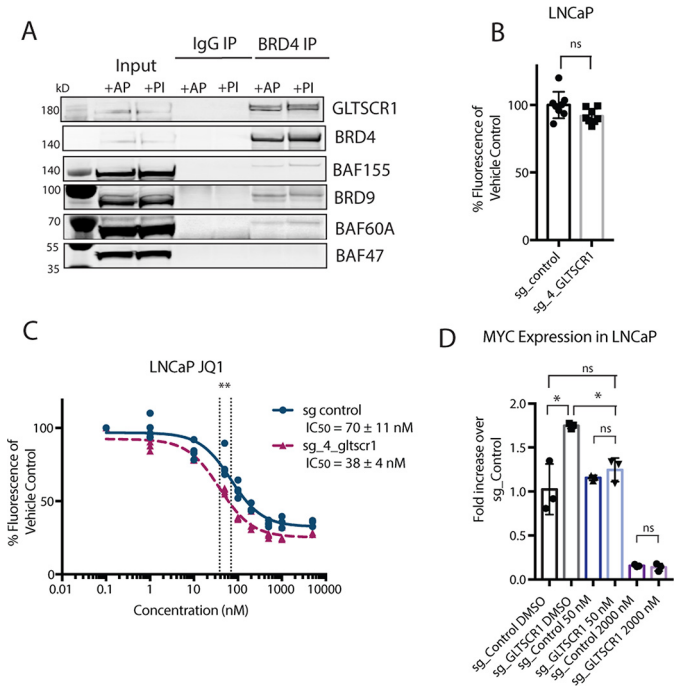

Figure 5. GLTSCR1 associates with BRD4 but is not required for BRD4-mediated *MYC* transcription in LNCaP cells. *A*, immunoprecipitation of BRD4 enriches GLTSCR1, BRD9, and BAF155 but not BAF/PBAF subunit BAF47. *AP*, lysates treated with alkaline phosphatase; *PI*, lysates treated with phosphatase inhibitors. *B*, proliferation measurement after 6 days of growth of LNCaP cells with *GLTSCR1* knockout using Alamar Blue. *Error bars*, means ± S.D. for $n = 6$ replicates. *C*, *GLTSCR1* knockout sensitized LNCaP to BET inhibitor JQ1. Cell numbers are approximated using Alamar Blue fluorescence. IC_{50} values are derived from curve fit calculations using GraphPad Prism and presented as means ± S.D. for $n = 4$ replicates. **, $p < 0.01$. *D*, *MYC* expression is up-regulated in *GLTSCR1* knockout LNCaP cells, which reverted back to basal levels upon 50 nM JQ1 treatment. *Error bars*, mean ± S.D. ($n = 3$ replicates). *, $p < 0.05$.

Our results also indicate a potential unexplored role for GBAF in BRD4-dependent function. Although several studies have noted the association between BRD4 and BRG1 (45), it has not been clear how they might be functionally related in cancer. For example, AML is dependent on both BRD4 (46, 47) and BRG1 (43, 47); however, their roles in AML transcriptional regulation are very different, making it difficult to determine the functional relevance of this association. We find that the association between BRD4 and BRG1 is specific to GLTSCR1, which will provide a framework for deciphering the functional relevance of this association in both normal and cancer settings. Further defining the importance of the association between GLTSCR1 and BRD4, as well as defining the general contribution of GBAF in chromatin targeting, nucleosome remodeling, and transcriptional regulation, will be critical for defining its contribution to human development and disease.

Experimental procedures

Cell lines and culture conditions

PC3 cells (American Type Culture Collection, Manassas, VA) were grown in F12K (Kaighn's modification) (Corning Mediatech, Inc., Manassas, VA) supplemented with 10% fetal bovine serum (JR Scientific, Inc., Woodland, CA), 100 units/ml penicillin and 100 g/ml streptomycin (Corning Mediatech, Inc.), and 2 mM L-alanyl-L-glutamine (Corning Glutagro™; Corning Mediatech, Inc.). HEK293T cells were cultured in DMEM (Corning Mediatech, Inc.) supplemented with 10% fetal bovine serum (JR Scientific, Inc.), 100 units/ml penicillin and 100 g/ml streptomycin (Corning Mediatech), 2 mM L-alanyl-L-glutamine (Corning Glutagro™; Corning Mediatech), and 1 mM sodium pyruvate (Corning Mediatech). NMuMG cells were cultured in DMEM (Corning Mediatech) containing 10% fetal bovine serum (JR Scientific, Inc.), 100 units/ml penicillin and 100 g/ml streptomycin (Corning Mediatech), 2 mM L-alanyl-L-glutamine (Corning Glutagro™; Corning Mediatech), 1 mM sodium pyruvate (Corning Mediatech), and 10 μg/ml insulin (Sigma). Mouse embryonic stem cell line E14 was cultured in DMEM (Corning Mediatech) supplemented with 15% fetal bovine serum (JR Scientific, Inc.), 100 units/ml penicillin and 100 g/ml streptomycin (Corning Mediatech), 2 mM L-alanyl-L-glutamine (Corning Glutagro™; Corning Mediatech), 1 mM sodium pyruvate (Corning Mediatech), 10 mM HEPES (HyClone Laboratories, Inc.), 1% MEM nonessential amino acids (Corning Mediatech), 1× 2-mercaptoethanol (Gibco), and 0.2% leukemia inhibitory factor-conditioned medium. E14 cells were plated onto gelatinized tissue culture plates without feeder layer. SVG p12 and T98 cell lines were grown in MEM (Corning Mediatech) supplemented with 10% fetal bovine serum (JR Scientific, Inc.), 100 units/ml penicillin and 100 g/ml streptomycin (Corning Mediatech), 2 mM L-alanyl-L-glutamine (Corning Glutagro™; Corning Mediatech), 1 mM sodium pyruvate (Corning Mediatech), and 1% MEM nonessential amino acids (Corning Mediatech). LNCaP cells were cultured in RPMI 1640 phenol-free medium with 10% fetal bovine serum (JR Scientific, Inc.), 100 units/ml penicillin and 100 g/ml streptomycin (Corning Mediatech), and 2 mM L-alanyl-L-glutamine (Corning Glutagro™; Corning Mediatech). Caki1 cells were cultured in McCoy's 5A medium (Corning Mediatech) with 10% fetal bovine serum (JR Scientific, Inc.), 100 units/ml penicillin and 100 g/ml streptomycin (Corning Mediatech), and 2 mM L-alanyl-L-glutamine (Corning Glutagro™; Corning Mediatech). THP1 cells were cultured in RPMI 1640 medium (Corning Mediatech) supplemented with 10% fetal bovine serum (JR Scientific, Inc.), 100 units/ml penicillin and 100 g/ml streptomycin (Corning Mediatech), 2 mM L-alanyl-L-glutamine (Corning Glutagro™; Corning Mediatech), and 1 × 2-mercaptoethanol (Gibco). All cell lines are incubated in 37 °C and 5% CO_2 atmosphere.

Antibodies

Antibodies used in the study are BRG1 (Abcam, ab110641, IP, and Western blotting), BAF60A (Bethyl, A301-594A, IP), BAF170 (Santa Cruz, sc-17838, IP, and Western blotting), GLTSCR1 (Santa Cruz, sc-515086, IP, and Western blotting), FLAG (Sigma–Aldrich, F1804), BRD4 (Bethyl, A301-985A50, IP), BRD9 (A303-781A IP and Western blotting), SS18 (Cell Signaling Technologies, 21792S, IP, and Western blotting), ARID1A (Santa Cruz, sc-32761, Western blotting), GLTSCR1L/BICRAL (Invitrogen, PA5-56126, Western blotting), BRD4 (Bethyl, A700-005-T, Western blotting), BRD7 (Santa Cruz, sc-376180, Western blotting), ARID2 (Bethyl, A302-230A, Western blotting), BAF155 (in-house, IP) BAF45D (in-house, IP, and Western blotting), BAF57 (Bethyl, A300-

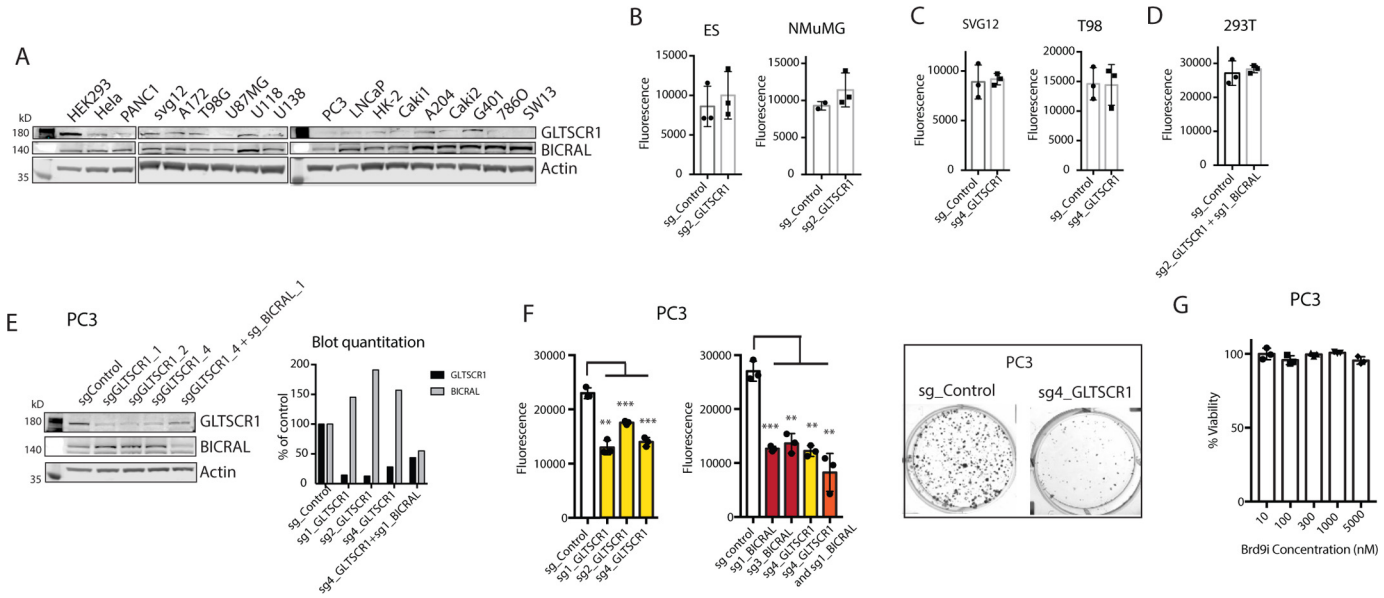

Figure 6. GLTSCR1 and BICRAL are expressed in most cell lines but are uniquely required for the viability of prostate cancer cell line PC3. *A*, immunoblot analysis of GLTSCR1 and BICRAL expression across a panel of cell lines. *B*, proliferation measurement after 6 days of growth of the non-transformed mouse cell lines mESCs and NMuMG with *Gltscr1* knockout using Alamar Blue. *C*, proliferation measurement after 6 days of growth of the transformed human astrocyte cell line SVGp12 and glioblastoma cell line T98G with *GLTSCR1* knockout using Alamar Blue. *D*, proliferation measurement after 6 days of growth of HEK293T cells with *GLTSCR1* and *BICRAL* knockout using Alamar Blue. *E*, validation of knockouts using multiple guide RNAs. *F*, *left panel*, Alamar Blue assay demonstrated that loss of *GLTSCR1* and *BICRAL* reduced the growth of PC3 cells 6 day after plating. Fluorescence values graphed (excitation, 560 nm; emission, 590 nm) represent the metric for cell number. *Error bars*, means ± S.D. ($n = 3$ biological replicates). **, $p < 0.01$; ***, $p < 0.001$ compared with control cells. *Right panel*, loss of GLTSCR1 reduced the clonogenic growth of prostate cell line PC3. *G*, PC3 cells did not display sensitivity to BRD9 inhibitor BI-7273 (IC_{50} of 275 nM) up to 10 μM treatment for 4 days. Cell number was approximated using Alamar Blue fluorescence ($n = 3$ biological replicates).

810A, IP, and Western blotting), BAF155 (Santa Cruz, sc-32763, Western blotting), BAF53A (Abcam, ab131272, Western blotting), BAF60A (Santa Cruz, sc-514400, Western blotting), PBRM1 (Bethyl, A301-590A, Western blotting), ARID1B (Bethyl, A301-047-T, Western blotting), BCL11A (Santa Cruz, sc-514842, IP and Western blotting), Actin (Santa Cruz, sc-47778, Western blotting), GAPDH (Santa Cruz, sc-137179, Western blotting), and α-tubulin (Santa Cruz, sc-8035, Western blotting).

Immunoblot analysis

Proteins from whole cells, nuclear extracts, salt extractions, or glycerol gradient sedimentation analyses were mixed with 4× lithium dodecyl sulfate sample buffer containing 10% 2-merchaptoethanol. The proteins were denatured for 5 min at 95 °C, separated on a 4–12% SDS-polyacrylamide gel, and transferred to a PVDF membrane (Immobilon FL, EMD Millipore, Billerica, MA). The membrane was blocked with 5% bovine serum albumin (VWR, Batavia, IL) in PBS containing 0.1% Tween 20 for 30 min at room temperature and then incubated in primary antibodies overnight at 4 °C. The primary antibodies were detected by incubating the membranes in goat anti-rabbit or goat anti-mouse secondary antibodies (LI-COR Biotechnology, Lincoln, NE) conjugated to IRDye 800CW or IRDye 680, respectively, for 1 h at room temperature, and the signals were visualized using Odyssey Clx imager (LI-COR Biotechnology).

Immunoprecipitation

The cells were harvested by trypsinization and washed once in ice-cold phosphate buffered saline (pH 7.2). The pellet was resuspended in buffer A (20 mM HEPES, pH 7.9, 25 mM KCl, 10% glycerol, 0.1% Nonidet P-40 with PMSF, aprotinin, leupeptin, and pepstatin) at a concentration of 20 million cells/ml. The cells were kept on ice for 5 min, and nuclei were isolated by centrifugation at 600 × *g* (Eppendorf Centrifuge 5810 R, Hamburg, Germany) for 10 min. Pelleted nuclei were washed once in buffer A without Nonidet P-40 and pelleted again. The nuclei pellet was resuspended in chromatin IP buffer (20 mM HEPES, pH 7.9, 150 mM NaCl, 1%Triton X-100, 7.5 mM $MgCl_2$, 0.1 mM $CaCl_2$). 4 units/ml Turbo DNase (Ambion, Inc., Foster City, CA) was added to extracts and rotated at 4 °C for 30 min. The extracts were cleared by centrifugation (Centrifuge 5424 R; Eppendorf, Hamburg, Germany) at 21,000 × *g* for 30 min. The cleared extract was precleared with normal IgG-conjugated (Santa Cruz, Dallas, TX) protein A/G magnetic beads (Pierce). One microgram specific IgG was used per 0.2 mg lysate for immunoprecipitation. After overnight incubation, immunocomplexes were captured using protein A/G magnetic beads following a 2-h incubation. The beads were washed twice in chromatin IP buffer and three times in high stringency wash buffer (20 mM HEPES, pH 7.9, 500 mM NaCl, 1% Triton X-100, 0.5% sodium deoxycholate, 1 mM EDTA). The proteins were eluted in 1× lithium dodecyl sulfate loading dye (Thermo Scientific) by boiling at 70 °C for 10 min. For urea denaturation followed by BRG1 IP, urea was added into nuclear lysates to final concentration of 0.5 or 2.5 M and incubated at 4 °C for 1 h. The lysates were then dialyzed against chromatin IP buffer for 50 min, precleared, and incubated with normal IgG or BRG1 antibodies. For on-bead alkaline phosphatase treatment during BRD4 IP, proteins were extracted in buffers with or without 1×

phosphatase inhibitor mixture 3 (Apexbio, Taiwan)/1 mM sodium orthovanadate and immunoprecipitated as described above. Following two washes in chromatin IP buffer, the beads were washed once in FastAP reaction buffer (Thermo Scientific, Waltham, MA) and incubated at 37 °C for 1 h with or without 10 units alkaline phosphatase. Reaction mixtures were removed, and the beads were washed in chromatin IP buffer twice more. The beads were then boiled and run on gel.

Glycerol gradient sedimentation analysis

30 million cells were collected by trypsinization, lysed in buffer A, and washed once with buffer A without Nonidet P-40. The nuclei were resuspended in buffer C (10 mM HEPES, pH 7.6, 3 mM $MgCl_2$, 100 mM KCl, 0.1 mM EDTA, 10% glycerol). 0.3 M ammonium sulfate was added on nuclei suspension and rotated at 4 °C for 30 min. Chromatin pellet was removed by ultracentrifugation at 150,000 × *g* for 30 min. 0.3 g/ml ammonium sulfate powder was added, and the supernatant was incubated on ice for 20 min. Proteins were precipitated by ultracentrifugation at 150,000 × *g* for 30 min. The protein pellet was resuspended in 100 μl of HEMG1000 buffer (25 mM HEPES, pH 7.6, 0.1 mM EDTA, 12.5 mM $MgCl_2$, 100 mM KCl) with protease inhibitors. 10–30% glycerol gradient was prepared using HEMG1000 buffer without glycerol and HEMG1000 buffer with 30% glycerol. Resuspended protein was layered over the top of 10–30% glycerol gradient (10 ml) and was fractionated by centrifugation at 40,000 rpm (XL-100K; Beckman Coulter, Brea, CA) for 16 h using SW32Ti rotor (Beckman Coulter). Twenty 500-μl fractions were collected sequentially from the top and used for immunoblot analysis.

RT-qPCR

RNA was extracted using TRIzol (Ambion, Inc.). cDNA was synthesized using Verso cDNA synthesis kit (Thermo Scientific) using random hexamers. Specific targets were amplified using SYBR Green Master Mix (Roche) and the following qPCR primers: *BICRAL* forward, 5′-GTTGCCACTCAGCTCCTAAA-3′; *BICRAL* reverse, 5′-CCTCCTGGTTGAACATCCTATC-3′; *GLTSCR1* forward, 5′-GATGAGGATGGGAGATGCTTAC-3′; *GLTSCR1* reverse, 5′-TCATAGAAGGCACTTTGGGC-3′; *BRG1* forward, 5′-TACAAGGACAGCAGCAGTGG-3′; *BRG1* reverse, 5′-TAGTACTCGGGCAGCTCCTT-3′; *BRD9* forward, 5′-GCCACGACTCCAGTTACTATG-3′; *BRD9* reverse, 5′-TCTCCTTCTCGGACTTCTTCT-3′; *MYCC* forward, 5′-AATGAAAAGGCCCCCAAGGTAGTTATCC-3′; and *MYCC* reverse, 5′-GTCGTTTCCGCAACAAGTCCTCTTC-3′.

Serial salt extraction assay

Serial salt extraction assay was performed as published with some modifications (48). Briefly, 5 million HEK293T cells were harvested by trypsinization and washed once with ice-cold PBS. The cells were lysed in modified buffer A (60 mM Tris, 60 mM KCl, 1 mM EDTA, 0.3 M sucrose, 0.5% Nonidet P-40, 1 mM DTT) with protease inhibitor, and nuclei were pelleted. The nuclei were then incubated in 200 μl of extraction buffer 0 (50 mM HEPES, pH 7.8, 0.3 M sucrose, 1 mM EGTA, 0.1% Triton X-100, 1 mM DTT, protease inhibitors) for 10 min and centrifuged at 7,000 × *g* for 5 min, and supernatant was collected as "0 mM fraction." The pellet was then resuspended in 200 μl of extraction buffer 100 (50 mM HEPES, pH 7.8, 0.3 M sucrose, 1 mM EGTA, 0.1% Triton X-100, 1 mM DTT, protease inhibitors, or 100 mM NaCl) and processed in the same manner to yield "100 mM fraction." Serial extraction was implemented with extraction buffers containing 200, 300, 400, and 500 mM NaCl. 20-μl aliquots from each fraction were mixed with 4× lithium dodecyl sulfate loading buffer and run for Western blotting.

Growth curve analysis and colony formation assay

For growth curve analysis, 500 or 1000 control or CRISPR-edited cells were plated in 96-well plates. After 6 days, culture medium was refreshed with 1:10 Alamar Blue reagent (Thermo Scientific) and incubated for 3 h. The fluorescence was measured with excitation at 560 nm and emission at 590 nm using BioTek plate reader. For colony formation assays, 100–200 cells were counted and plated on 6-well plates and allowed to form colonies for 10–15 days. Culture medium was removed and washed twice in ice-cold PBS. Then cells were fixed in 100% methanol for 10 min at −20 °C. Methanol was removed, and fixed cells were incubated in 0.5% crystal violet (prepared in 25% methanol) for 10 min at room temperature. Excess dye was removed by tap water washes until background was cleared. The images were acquired using Chemi-Doc (Bio-Rad).

ATPase assay

ATPase assay was performed based on previously published procedure (49) using ADP-GloMax Assay (Promega, Madison, WI) with minor modifications. 25 million (for BRG1 IP) or 100 million (for GLTSCR1 IP) HEK293T cells were lysed in buffer A. Pelleted nuclei were extracted for 30 min at 4 °C using lysis buffer (50 mM Tris, pH 8.0, 150 mM NaCl and 0.2% IPEGAL CA-630, 1 mM DTT, 0.2 mM PMSF, and protease inhibitors) at a ratio of 50 million cells/400 μl of buffer. The extract was cleared at 21,000 × *g* for 1 h. One microliter of BRG1 antibody, 10 μl of GLTSCR1 antibody or corresponding amount of normal IgG antibodies were added per 400 μl of cleared extract for overnight immunoprecipitation at 4 °C in a rotating wheel. 10 μl (for BRG1 and rabbit IgG) or 25 μl (for GLTSCR1 and mouse IgG) protein A/G magnetic beads were added to each of 400-μl IP samples and rotated for 2 h more. The beads were washed twice in lysis buffer and then in wash buffer (10 mM Tris, pH 7.5, 50 mM NaCl, 5 mM $MgCl_2$, 1 mM DTT, and protease inhibitors). The number of beads were adjusted such that material from 25 million (for BRG1 IP) or 100 million (for GLTSCR1 IP) HEK293T cells were included per ATPase reaction. The beads were resuspended in 25 μL of reaction buffer (10 mM Tris, pH 7.5, 50 mM NaCl, 5 mM $MgCl_2$, 20% glycerol, 1 mg/ml BSA, 4 mM ATP, 0.5 μg/μl ssDNA, 1 mM DTT, and protease inhibitors and incubated at 37 °C for 1 h on a shaker. The beads were separated, and the reactions were transferred to 96-well opaque white plate. 25 μl of ADP-Glo reagent were added per well and gently shaken for 1 h at

Table 1
Short guide RNA sequences

	Sequence (5′ → 3′)	Organism	Reference
sgGLTSCR1_1	GGTTGGGCTCTGGGTTCAGG	Human	
sgGLTSCR1_2	CAACCAGCCGGCCCCCAGTG	Human	
sgGLTSCR1_3	GGACCAGTGGCGACGAGCCG	Human	Ref. 50
sgGLTSCR1_4	GCAGAACCTGACGTTCATGG	Human	Ref. 50
sgBICRAL_1	GTAAGCAACCAGCTTGGAGA	Human	
sgBICRAL_2	GAAAGTGGCAGTCCATCACT	Human	
sgBICRAL_3	GTTCATCTTCAAGAAACTGG	Human	
sgGltscr1_1	ACCCTACAGCCCGCTGACAA	Mouse	
sgGltscr1_2	CCCCATTGTCAGCGGGCTGT	Mouse	
sgGltscr1_3	CCCATTGTCAGCGGGCTGTA	Mouse	
sgCTRL	GTAGCGAACGTGTCCGGCGT	Human/mouse	Ref. 50

room temperature. 50 μl of detection reagent were added per well and further shaken for 1 h. Luminescence was detected at 1-s integration time.

Cytotoxicity analysis

10,000 (LNCaP) or 5,000 (PC3) cells were plated in 100 μl on 96-well plate. The next day, JQ1, OTX015, BI-7372, or DMSO was added, and the cells were further incubated for 4 days. The cells were treated with Alamar Blue reagent for 3 h more, and absorbance values were recorded at 570 and 600 nm. Percent viability was expressed relative to the DMSO-treated control cells.

Generation of CRISPR/CAS9-mediated knockout

Short guide RNA (sgRNA) sequences were retrieved from (50) or designed using MIT CRISPR Tool (http://crispr.mit.edu/)[3] or Synthego CRISPR design tool (https://design.synthego.com/)[3] (Table 1). The top and bottom strands of the sgRNA were ordered as single-stranded DNA oligonucleotides from Sigma–Aldrich and cloned into lenticrispr v2.0 (a gift from Feng Zhang Addgene plasmid no. 52961) following the well-established protocol (51). The vector was packaged into lentivirus using HEK293T cells, and the viral particles were concentrated by ultracentrifugation, and cell lines were transduced with concentrated virus. Stable lines were generated by puromycin selection. For *Gltscr1* KO mouse ESCs, clonal lines were generated.

BICRAL cloning and overexpression

BICRAL ORF was purchased from Novogen (catalog no. 762821-2). The ORF was amplified with in-frame C-terminal FLAG tag and 20-bp flanking sequences at both ends with homology to vector using Clontech HiFi PCR premix kit (Takara, USA) and cloned into EcoRI-digested TetO-FUW (a gift from Rudolf Jaenisch Addgene plasmid no. 20323) using ligation-free In-Fusion HD cloning kit (Takara). The construct was packaged into lentivirus and delivered into target cells together with pLenti CMV rtTA3 Hygro (w785-1) (a gift from Eric Campeau Addgene plasmid no. 26730) for tetracycline inducible expression. The cells were selected with puromycin and hygromycin B. For BICRAL expression, HEK293T cells were treated with doxycycline for 6 days.

[3] Please note that the JBC is not responsible for the long-term archiving and maintenance of this site or any other third party hosted site.

Author contributions—A. A. and E. C. D. conceptualization; A. A. and E. C. D. data curation; A. A. and E. C. D. formal analysis; A. A. and E. C. D. validation; A. A. and E. C. D. investigation; A. A. and E. C. D. visualization; A. A. and E. C. D. methodology; A. A. and E. C. D. writing-original draft; A. A. and E. C. D. writing-review and editing; E. C. D. resources; E. C. D. software; E. C. D. supervision; E. C. D. funding acquisition; E. C. D. project administration.

Acknowledgments—We thank the Purdue University Proteomics Facility for assistance with the initial mass spectrometry and Gerald Crabtree for generously providing in house antibodies for BAF155 and BAF45D.

References

1. Wang, W., Côté, J., Xue, Y., Zhou, S., Khavari, P. A., Biggar, S. R., Muchardt, C., Kalpana, G. V., Goff, S. P., Yaniv, M., Workman, J. L., and Crabtree, G. R. (1996) Purification and biochemical heterogeneity of the mammalian SWI-SNF complex. *EMBO J.* **15,** 5370–5382 Medline
2. Hargreaves, D. C., and Crabtree, G. R. (2011) ATP-dependent chromatin remodeling: genetics, genomics and mechanisms. *Cell Res.* **21,** 396–420 CrossRef Medline
3. Dhalluin, C., Carlson, J. E., Zeng, L., He, C., Aggarwal, A. K., and Zhou, M. M. (1999) Structure and ligand of a histone acetyltransferase bromodomain. *Nature* **399,** 491–496 CrossRef Medline
4. Owen, D. J., Ornaghi, P., Yang, J. C., Lowe, N., Evans, P. R., Ballario, P., Neuhaus, D., Filetici, P., and Travers, A. A. (2000) The structural basis for the recognition of acetylated histone H4 by the bromodomain of histone acetyltransferase Gcn5p. *EMBO J.* **19,** 6141–6149 CrossRef Medline
5. Ronan, J. L., Wu, W., and Crabtree, G. R. (2013) From neural development to cognition: unexpected roles for chromatin. *Nat. Rev. Genet.* **14,** 347–359 CrossRef Medline
6. Zinzalla, G. (2016) A new way forward in cancer drug discovery: inhibiting the SWI/SNF chromatin remodelling complex. *ChemBioChem.* **17,** 677–682 CrossRef Medline
7. Kalpana, G. V., Marmon, S., Wang, W., Crabtree, G. R., and Goff, S. P. (1994) Binding and stimulation of HIV-1 integrase by a human homolog of yeast transcription factor SNF5. *Science* **266,** 2002–2006 CrossRef Medline
8. Rafati, H., Parra, M., Hakre, S., Moshkin, Y., Verdin, E., and Mahmoudi, T. (2011) Repressive LTR nucleosome positioning by the BAF complex is required for HIV latency. *PLoS Biol.* **9,** e1001206 CrossRef Medline
9. Mathies, L. D., Aliev, F., Davies, A. G., COGA Investigators, Dick, D. M., and Bettinger, J. C. (2017) Variation in SWI/SNF chromatin remodeling complex proteins is associated with alcohol dependence and antisocial behavior in human populations. *Alcohol. Clin. Exp. Res.* **41,** 2033–2040 CrossRef Medline
10. Mathies, L. D., Blackwell, G. G., Austin, M. K., Edwards, A. C., Riley, B. P., Davies, A. G., and Bettinger, J. C. (2015) SWI/SNF chromatin remodeling regulates alcohol response behaviors in *Caenorhabditis elegans* and is associated with alcohol dependence in humans. *Proc. Natl. Acad. Sci. U.S.A.* **112,** 3032–3037 CrossRef Medline

11. Hang, C. T., Yang, J., Han, P., Cheng, H.-L., Shang, C., Ashley, E., Zhou, B., and Chang, C.-P. (2010) Chromatin regulation by Brg1 underlies heart muscle development and disease. *Nature* **466,** 62–67 CrossRef Medline
12. Wu, J. I. (2012) Diverse functions of ATP-dependent chromatin remodeling complexes in development and cancer. *Acta Biochim. Biophys. Sin.* (*Shanghai*) **44,** 54–69
13. Lopes Cardoso, D., and Sharpe, C. (2017) Relating protein functional diversity to cell type number identifies genes that determine dynamic aspects of chromatin organisation as potential contributors to organismal complexity. *PLoS One* **12,** e0185409 CrossRef Medline
14. Mani, U., S, A. S., Goutham, R. N. A., and Mohan, S. S. (2017) SWI/SNF Infobase: an exclusive information portal for SWI/SNF remodeling complex subunits. *PLoS One* **12,** e0184445 CrossRef Medline
15. Wu, J. I., Lessard, J., and Crabtree, G. R. (2009) Understanding the words of chromatin regulation. *Cell* **136,** 200–206 CrossRef Medline
16. Phelan, M. L.., Sif, S., Narlikar, G. J., and Kingston, R. E. (1999) Reconstitution of a core chromatin remodeling complex from SWI/SNF subunits. *Mol. Cell* **3,** 247–253 CrossRef Medline
17. Ho, L., and Crabtree, G. R. (2010) Chromatin remodelling during development. *Nature* **463,** 474–484 CrossRef Medline
18. Middeljans, E., Wan, X., Jansen, P. W., Sharma, V., Stunnenberg, H. G., and Logie, C. (2012) SS18 together with animal-specific factors defines human BAF-type SWI/SNF complexes. *PLoS One* **7,** e33834 CrossRef Medline
19. Staahl, B. T., Tang, J., Wu, W., Sun, A., Gitler, A. D., Yoo, A. S., and Crabtree, G. R. (2013) Kinetic analysis of npBAF to nBAF switching reveals exchange of SS18 with CREST and integration with neural developmental pathways. *J. Neurosci.* **33,** 10348–10361 CrossRef Medline
20. Raab, J. R., Resnick, S., and Magnuson, T. (2015) Genome-wide transcriptional regulation mediated by biochemically distinct SWI/SNF complexes. *PLoS Genet.* **11,** e1005748 CrossRef Medline
21. Mathur, R., Alver, B. H., San Roman, A. K., Wilson, B. G., Wang, X., Agoston, A. T., Park, P. J., Shivdasani, R. A., and Roberts, C. W. (2017) ARID1A loss impairs enhancer-mediated gene regulation and drives colon cancer in mice. *Nat. Genet.* **49,** 296–302 CrossRef Medline
22. Kelso, T. W. R., Porter, D. K., Amaral, M. L., Shokhirev, M. N., Benner, C., and Hargreaves, D. C. (2017) Chromatin accessibility underlies synthetic lethality of SWI/SNF subunits in ARID1A-mutant cancers. *eLife* **6,** e30506 Medline
23. Helming, K. C., Wang, X., Wilson, B. G., Vazquez, F., Haswell, J. R., Manchester, H. E., Kim, Y., Kryukov, G. V., Ghandi, M., Aguirre, A. J., Jagani, Z., Wang, Z., Garraway, L. A., Hahn, W. C., and Roberts, C. W. (2014) ARID1B is a specific vulnerability in ARID1A-mutant cancers. *Nat. Med.* **20,** 251–254 CrossRef Medline
24. Wurster, A. L., Precht, P., Becker, K. G., Wood, W. H., 3rd, Zhang, Y., Wang, Z., and Pazin, M. J. (2012) IL-10 transcription is negatively regulated by BAF180, a component of the SWI/SNF chromatin remodeling enzyme. *BMC Immunol.* **13,** 9 CrossRef Medline
25. Mayes, K., Qiu, Z., Alhazmi, A., and Landry, J. W. (2014) ATP-dependent chromatin remodeling complexes as novel targets for cancer therapy. *Adv. Cancer Res.* **121,** 183–233 CrossRef Medline
26. Hohmann, A. F., and Vakoc, C. R. (2014) A rationale to target the SWI/SNF complex for cancer therapy. *Trends Genet.* **30,** 356–363 CrossRef Medline
27. Ho, L., Ronan, J. L., Wu, J., Staahl, B. T., Chen, L., Kuo, A., Lessard, J., Nesvizhskii, A. I., Ranish, J., and Crabtree, G. R. (2009) An embryonic stem cell chromatin remodeling complex, esBAF, is essential for embryonic stem cell self-renewal and pluripotency. *Proc. Natl. Acad. Sci. U.S.A.* **106,** 5181–5186 CrossRef Medline
28. Hein, M. Y., Hubner, N. C., Poser, I., Cox, J., Nagaraj, N., Toyoda, Y., Gak, I. A., Weisswange, I., Mansfeld, J., Buchholz, F., Hyman, A. A., and Mann, M. (2015) A human interactome in three quantitative dimensions organized by stoichiometries and abundances. *Cell* **163,** 712–723 CrossRef Medline
29. Huttlin, E. L., Bruckner, R. J., Paulo, J. A., Cannon, J. R., Ting, L., Baltier, K., Colby, G., Gebreab, F., Gygi, M. P., Parzen, H., Szpyt, J., Tam, S., Zarraga, G., Pontano-Vaites, L., Swarup, S., *et al.* (2017) Architecture of the human interactome defines protein communities and disease networks. *Nature* **545,** 505–509 CrossRef Medline
30. Uhlén, M., Fagerberg, L., Hallström, B. M., Lindskog, C., Oksvold, P., Mardinoglu, A., Sivertsson, Å., Kampf, C., Sjöstedt, E., Asplund, A., Olsson, I., Edlund, K., Lundberg, E., Navani, S., Szigyarto, C. A., *et al.* (2015) Tissue-based map of the human proteome. *Science* **347,** 1260419 CrossRef Medline
31. Porter, E. G., and Dykhuizen, E. C. (2017) Individual bromodomains of polybromo-1 contribute to chromatin association and tumor suppression in clear cell renal carcinoma. *J. Biol. Chem.* **292,** 2601–2610 CrossRef Medline
32. Rahman, S., Sowa, M. E., Ottinger, M., Smith, J. A., Shi, Y., Harper, J. W., and Howley, P. M. (2011) The Brd4 extraterminal domain confers transcription activation independent of pTEFb by recruiting multiple proteins, including NSD3. *Mol. Cell. Biol.* **31,** 2641–2652 CrossRef Medline
33. Crowe, B. L., Larue, R. C., Yuan, C., Hess, S., Kvaratskhelia, M., and Foster, M. P. (2016) Structure of the Brd4 ET domain bound to a C-terminal motif from γ-retroviral integrases reveals a conserved mechanism of interaction. *Proc. Natl. Acad. Sci. U.S.A.* **113,** 2086–2091 CrossRef Medline
34. Wu, S.-Y., Lee, A.-Y., Lai, H.-T., Zhang, H., and Chiang, C.-M. (2013) Phospho switch triggers Brd4 chromatin binding and activator recruitment for gene-specific targeting. *Mol. Cell* **49,** 843–857 CrossRef Medline
35. Asangani, I. A., Dommeti, V. L., Wang, X., Malik, R., Cieslik, M., Yang, R., Escara-Wilke, J., Wilder-Romans, K., Dhanireddy, S., Engelke, C., Iyer, M. K., Jing, X., Wu, Y.-M., Cao, X., Qin, Z. S., *et al.* (2014) Therapeutic targeting of BET bromodomain proteins in castration-resistant prostate cancer. *Nature* **510,** 278–282 CrossRef Medline
36. Shen, C., Ipsaro, J. J., Shi, J., Milazzo, J. P., Wang, E., Roe, J.-S., Suzuki, Y., Pappin, D. J., Joshua-Tor, L., and Vakoc, C. R. (2015) NSD3-Short is an adaptor protein that couples BRD4 to the CHD8 chromatin remodeler. *Mol. Cell* **60,** 847–859 CrossRef Medline
37. Hohmann, A. F., Martin, L. J., Minder, J. L., Roe, J.-S., Shi, J., Steurer, S., Bader, G., McConnell, D., Pearson, M., Gerstberger, T., Gottschamel, T., Thompson, D., Suzuki, Y., Koegl, M., and Vakoc, C. R. (2016) Sensitivity and engineered resistance of myeloid leukemia cells to BRD9 inhibition. *Nat. Chem. Biol.* **12,** 672–679 CrossRef Medline
38. Dickinson, M. E., Flenniken, A. M., Ji, X., Teboul, L., Wong, M. D., White, J. K., Meehan, T. F., Weninger, W. J., Westerberg, H., Adissu, H., Baker, C. N., Bower, L., Brown, J. M., Caddle, L. B., Chiani, F., *et al.* (2016) High-throughput discovery of novel developmental phenotypes. *Nature* **537,** 508–514 CrossRef Medline
39. Forbes, S. A., Bindal, N., Bamford, S., Cole, C., Kok, C. Y., Beare, D., Jia, M., Shepherd, R., Leung, K., Menzies, A., Teague, J. W., Campbell, P. J., Stratton, M. R., and Futreal, P. A. (2011) COSMIC: mining complete cancer genomes in the Catalogue of Somatic Mutations in Cancer. *Nucleic Acids Res.* **39,** D945–D950 CrossRef Medline
40. Sun, A., Tawfik, O., Gayed, B., Thrasher, J. B., Hoestje, S., Li, C., and Li, B. (2007) Aberrant expression of SWI/SNF catalytic subunits BRG1/BRM is associated with tumor development and increased invasiveness in prostate cancers. *Prostate* **67,** 203–213 CrossRef Medline
41. Wang, X., Sansam, C. G., Thom, C. S., Metzger, D., Evans, J. A., Nguyen, P. T., and Roberts, C. W. (2009) Oncogenesis caused by loss of the SNF5 tumor suppressor is dependent on activity of BRG1, the ATPase of the SWI/SNF chromatin remodeling complex. *Cancer Res.* **69,** 8094–8101 CrossRef Medline
42. Krämer, K. F., Moreno, N., Frühwald, M. C., and Kerl, K. (2017) BRD9 inhibition, alone or in combination with cytostatic compounds as a therapeutic approach in rhabdoid tumors. *Int. J. Mol. Sci.* **18,** E1537 Medline
43. Shi, J., Whyte, W. A., Zepeda-Mendoza, C. J., Milazzo, J. P., Shen, C., Roe, J.-S., Minder, J. L., Mercan, F., Wang, E., Eckersley-Maslin, M. A., Campbell, A. E., Kawaoka, S., Shareef, S., Zhu, Z., Kendall, J., *et al.* (2013) Role of SWI/SNF in acute leukemia maintenance and enhancer-mediated Myc regulation. *Gene Dev.* **27,** 2648–2662 CrossRef Medline
44. Martin, L. J., Koegl, M., Bader, G., Cockcroft, X.-L., Fedorov, O., Fiegen, D., Gerstberger, T., Hofmann, M. H., Hohmann, A. F., Kessler, D., Knapp,

S., Knesl, P., Kornigg, S., Müller, S., Nar, H., *et al.* (2016) Structure-based design of an *in vivo* active selective BRD9 inhibitor. *J. Med. Chem.* **59,** 4462–4475 CrossRef Medline

45. Conrad, R. J., Fozouni, P., Thomas, S., Sy, H., Zhang, Q., Zhou, M.-M., and Ott, M. (2017) The short isoform of BRD4 promotes HIV-1 latency by engaging repressive SWI/SNF chromatin-remodeling complexes. *Mol. Cell* **67,** 1001–1012 CrossRef Medline
46. Zuber, J., Shi, J., Wang, E., Rappaport, A. R., Herrmann, H., Sison, E. A., Magoon, D., Qi, J., Blatt, K., Wunderlich, M., Taylor, M. J., Johns, C., Chicas, A., Mulloy, J. C., Kogan, S. C., *et al.* (2011) RNAi screen identifies Brd4 as a therapeutic target in acute myeloid leukaemia. *Nature* **478,** 524–528 CrossRef Medline
47. Shi, J., Wang, E., Milazzo, J. P., Wang, Z., Kinney, J. B., and Vakoc, C. R. (2015) Discovery of cancer drug targets by CRISPR-Cas9 screening of protein domains. *Nat. Biotechnol.* **33,** 661–667 CrossRef Medline
48. Porter, E. G., Connelly, K. E., and Dykhuizen, E. C. (2017) Sequential salt extractions for the analysis of bulk chromatin binding properties of chromatin modifying complexes. *J. Vis. Exp.* **128,** 10.3791/55369 CrossRef Medline
49. Stanton, B. Z., Hodges, C., Crabtree, G. R., and Zhao, K. (2017) *A General Non-radioactive ATPase Assay for Chromatin Remodeling Complexes*, John Wiley & Sons, Inc., Hoboken, NJ
50. Wang, T., Wei, J. J., Sabatini, D. M., and Lander, E. S. (2014) Genetic screens in human cells using the CRISPR-Cas9 system. *Science* **343,** 80–84 CrossRef Medline
51. Ran, F. A., Hsu, P. D., Wright, J., Agarwala, V., Scott, D. A., and Zhang, F. (2013) Genome engineering using the CRISPR-Cas9 system. *Nat. Protoc.* **8,** 2281–2308 CrossRef Medline